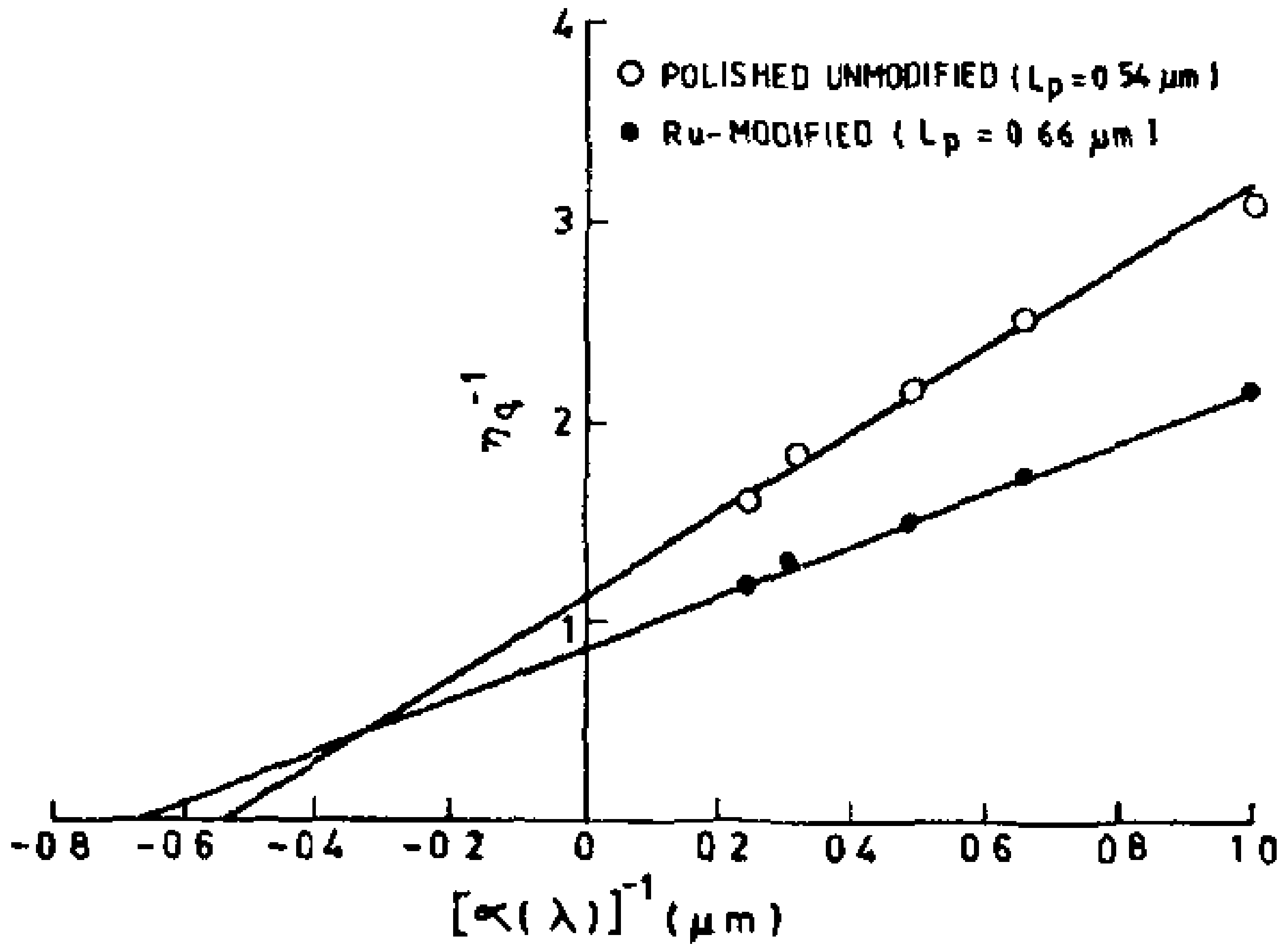

Figure 2. Plot of η_q^{-1} vs $\alpha(\lambda)^{-1}$ showing increased diffusion length (L_p) estimated from intercept. The $\alpha(\lambda)$ values were obtained from ref. 7 for 600 nm $\leq \lambda \geq$ 800 nm.

surface, i.e. $Z = 0$, it is found that increase in L_{eff} from 0.54 μm to 0.66 μm may be attributed to a reduction in S from 5.0×10^5 cm sec^{-1} to 2.65×10^5 cm sec^{-1}.

The solar cell I–V characteristics were obtained using a 1.5 kW tungsten-halogen lamp whose intensity was calibrated using a standard silicon cell. Figure 3 shows the photo I–V curves [average of anodic (I_{sc} to V_{oc}) and cathodic (V_{oc} to I_{sc}) scan] of polished and Ru-modified samples. When polished GaAs (exposed area = 3 mm × 3 mm) was dipped in 1 M KOH 0.1 M Te^{2-}/Te$_x^{2-}$ it showed (Figure 3, curve a) a conversion efficiency (η) of 7.81% with J_{sc} = 17.37 mA cm^{-2}, V_{oc} = 0.90 V, fill factor (FF) = 0.50 under AM1 condition. Exposure of the etched GaAs to Ru^{3+} ions yielded (Figure 3, curve b) better I–V properties with V_{oc} = 0.97 V, J_{sc} = 20.30 mA cm^{-2}, FF = 0.62, η = 12.2%. This V_{oc} value is the highest for GaAs PEC cells in an aqueous solution reported to date under AM1 condition. The improved FF from 0.50 to 0.62 may be attributed to reduced surface recombination at the photoanode as evident from lower ideality factor. It was also observed that photoanodes with smaller area (2 mm × 2 mm) showed (Figure 3, curve c) higher efficiency, η = 14.12%, with increased J_{sc} = 23.49 mA cm^{-2} owing to better charge transfer. The cells were found to be stable over 2–3 days.

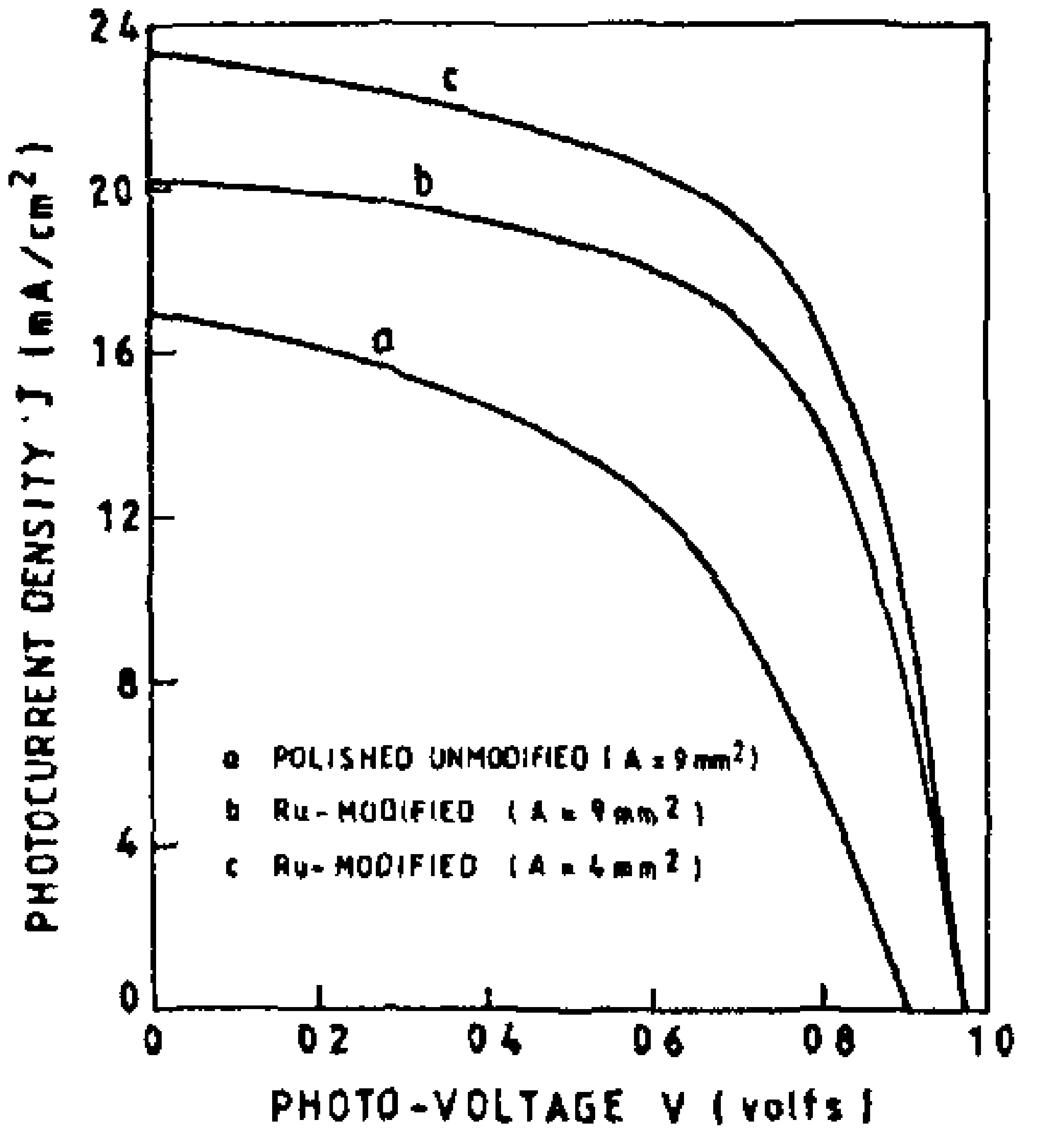

Figure 3. Photocurrent-voltage characteristics of n-GaAs photoanode in 1 M KOH 0.1 M Na$_2$Te/Na$_2$Te$_x$ graphite redox-electrolyte system under AM1 condition a η = 7.81%, b. η = 12.20%, c η = 14.12%

1. Parkinson, B A., Heller, A. and Miller, B., *Appl Phys. Lett.*, 1978, **33**, 521.
2. Bose, D. N., Basu, S., Mandal, K. C. and Mazumdar, D., *Appl Phys. Lett.*, 1986, **48**, 472.
3. Bose, D. N., Ramprakash, Y. and Basu, S., *J. Electrochem Soc*, 1984, **130**, 850.
4. Mandal, K. C., Basu, S. and Bose, D. N, *Solar Cells*, 1984, **18**, 25
5. Jastrzebski, L, Logowski, J and Gatos, H. C., *Appl. Phys Lett.*, 1975, **27**, 537.
6. Nelson, R. J., Williams, J. S., Leamy, H. J., Miller, B., Casey, H. C., Parkinson, B. A. and Heller, A, *Appl. Phys. Lett.*, 1980, **36**, 76.
7. Cardona, M, *Semiconductors and Semimetals*, (ed. Willardson, R. K. and Beer, A. C.), Academic, New York, 1972, vol. 8, pp. 134.

ACKNOWLEDGEMENTS We are grateful to the Department of Non-Conventional Energy Sources for a project under Chemtrapse which made this work possible.

Received 9 September 1991; accepted 4 October 1991

Highly saline fluid inclusions in Chamundi granite, South India

C. Srikantappa, K. N. Prakash Narasimha and H. T. Basavarajappa*

Department of Geology, University of Mysore, Manasagangotri, Mysore 570 006, India
*Mineralogical Institute, University of Mysore, Manasagangotri, Mysore 570 006, India

Fluid inclusions in minerals and rock represent a potentially valuable source of information about the composition and density of fluids present during the formation and evolution of rocks. Our preliminary studies on Chamundi granite have indicated presence of *highly saline inclusions (up to 50–60 wt.% NaCl equivalent)* as well as low-salinity inclusions (8 to 22 wt.% NaCl equivalent). Data on temperature of homogenization suggest that they represent remnant fluids of magmatic origin trapped in minerals.

STUDIES on fluid inclusions in granitic rocks have shown the presence of H$_2$O-rich, aqueous and melt inclusions[1]. Presence of CO$_2$-rich inclusions and CO$_2$

H_2O inclusions in granites, and of carbonic inclusions in Closepet granite of metasomatic origin[2] have also been reported. Here we report preliminary results obtained on fluid-inclusion characteristics of Chamundi granite near Mysore city.

Chamundi granite, an anorogenic pluton, is a prominent landmark in Mysore city (lat. 12° 20′ N, long 76° 40′ E), rising 1057 m above MSL. This granite intrudes into the gneisses (Peninsular Gneiss) and schists belonging to the Sargur Group (> 3.0 Gyr old). The granite exhibits sharp contact with the country rocks and sends out tongues and veins into the gneiss. The granite cuts across regional foliation of the country rocks of N 10–20° E. Field, structural and geochemical data have shown that Chamundi granite is a grey to pink granite of magmatic origin[3,4].

The medium- to coarse-grained Chamundi granite shows no oriented fabric. It is predominantly composed of pink granite (K-feldspar + quartz + biotite + plagioclase + zircon), with a minor grey-granitic component (quartz, plagioclase + K-feldspar + biotite). Numerous quartz and aplite veins are seen cutting across both pink and grey granites.

We studied doubly polished sections collected from pink granite, grey granite and quartz veins. Good, measurable inclusions were noticed mainly in quartz grains of the samples studied. The fluid inclusions vary in size from 5 μm to 15 μm and are generally randomly oriented within the quartz grains, indicating their primary nature[1]. Two types of fluid inclusions were noticed, viz. (i) biphase low-salinity H_2O-rich inclusions, and (ii) high-salinity halite-bearing inclusions. The biphase H_2O-rich inclusions are commonly noticed in quartz veins and are less common in pink and grey granites. They show presence of a liquid and a vapour phase at room temperature. The halite-bearing inclusions are mainly confined to pink granites. They vary in size from 5 μm to 15 μm and are irregular to oval in shape. They do not show any orientation and thus are considered to be primary in origin. These fluid inclusions contain a cubic, isotropic daughter mineral, identified as halite. These inclusions, apart from halite cubes ranging in size from 3 μm to 10 μm, contain a liquid phase and a vapour phase (Figure 1).

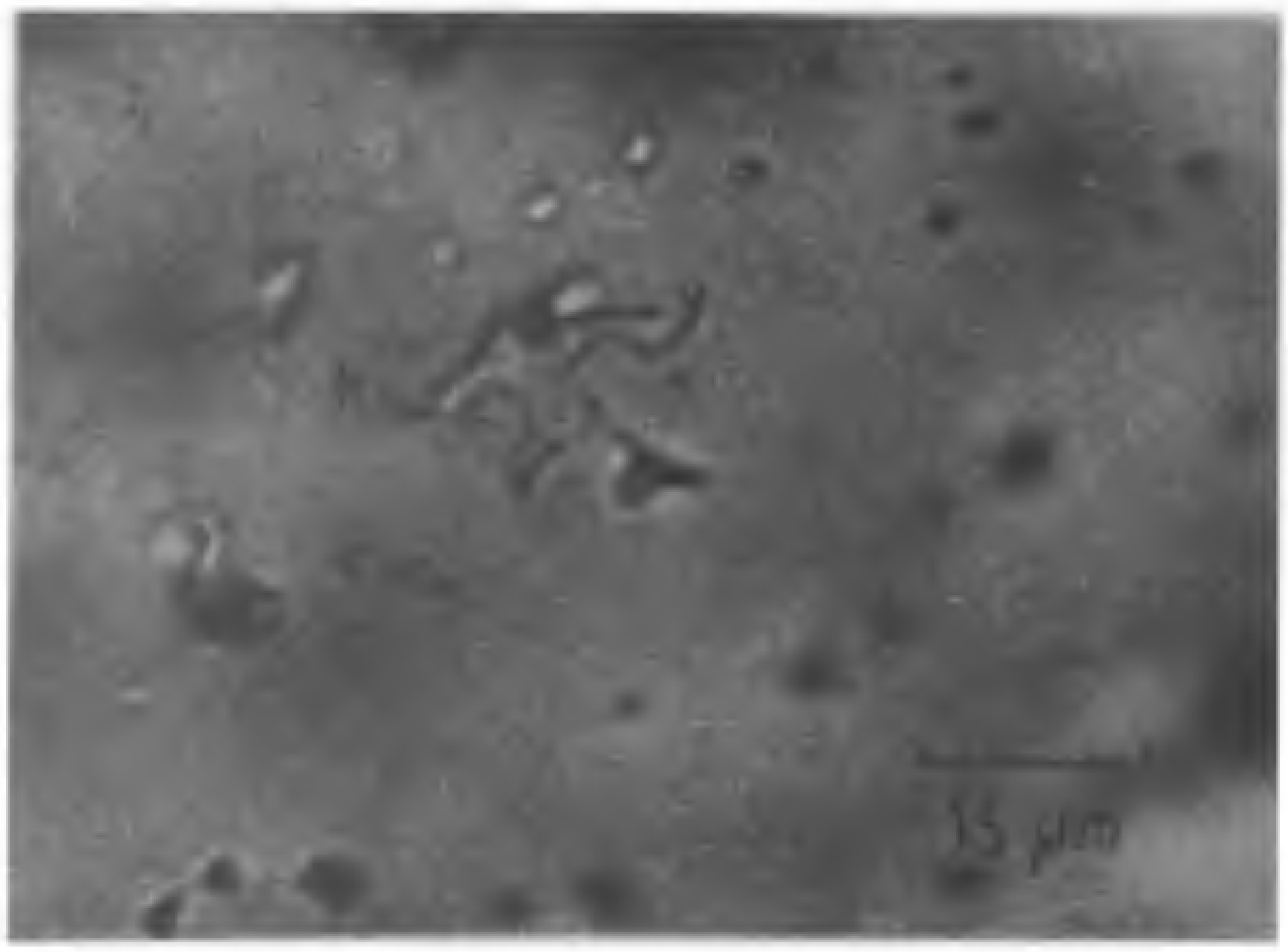

Figure 1. Halite-bearing fluid inclusion in a quartz grain.

Freezing-and-heating measurements of fluid inclusions were carried out using a Chaixmeca microthermometry stage, which was calibrated with various chemicals (E. Merck). Figure 2,*a* shows temperature of first melting (T_m) of ice crystals in fluid inclusions obtained from pink granite, grey granite and quartz vein. Biphase inclusions in pink granites show temperature of melting in the range from −1°C to −6°C, indicating low salinity values of 8 to 9 wt% NaCl equivalent. Temperature of homogenization (T_h, Figure 2,*b*) varies from 200°C to 260°C, with maximum values between 220°C and 240°C, yielding density values of 0.845 to 0.825 g cm^{-3} (ref. 5). Fluid inclusions in quartz veins show T_m between −12°C and −20°C, indicating salinity values of 21 to 22 wt% NaCl equivalent[6]. Temperature of homogenization (T_h) of the liquid phase for these inclusions varies from 120°C to 200°C, with maximum values in the range of 160°C to 180°C, giving density values of 1.103 and 1.101 g cm^{-3} (ref. 6). Halite-bearing inclusions when heated show homogenization of vapour phase into liquid phase in the beginning and then melting of halite crystal at higher temperature. Temperature of melting of halite crystal (T_m halite, Figure 2,*c*) varies between 400°C and 550°C, with maximum values between 500°C and 550°C, yielding higher salinity values of 55–60 wt% NaCl equivalent[6].

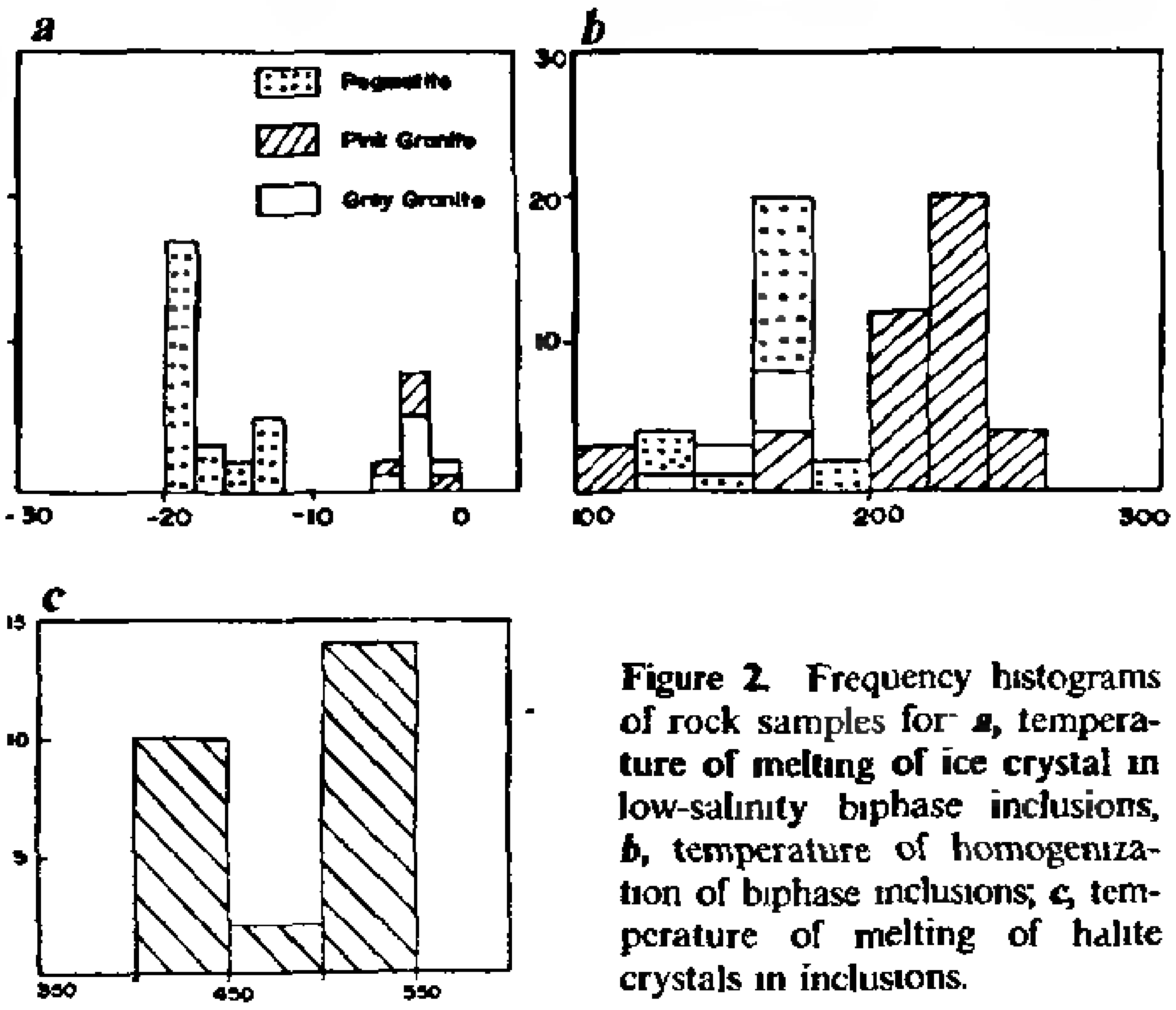

Figure 2. Frequency histograms of rock samples for *a*, temperature of melting of ice crystal in low-salinity biphase inclusions, *b*, temperature of homogenization of biphase inclusions; *c*, temperature of melting of halite crystals in inclusions.

These preliminary studies on Chamundi granite show the presence of highly saline fluids associated with pink granites. The present data do not permit a definite conclusion regarding the origin of these fluids, whether they represent primary magmatic water related to cooling history of the granite or resulted from late-stage interaction between the solid rock and deep circulating meteoric water. On the basis of the random orientation of these inclusions and their temperature of homogenization and high salinity, we suggest that they are remnants of magmatic fluids. Inclusions with low salinity associated with quartz veins represent a more evolved stage of fluid entrapment.

1. Roedder, E., *Rev. Mineral., Mineral Soc. Am.*, 1984, **12**, 644.
2. Newton, R. C., in *Fluid-Rock Interactions During Metamorphism*, (eds Walther, J. V. and Wood, B. J.), Springer, New York, 1986, pp. 36–59.
3. Jayaram, B., *Rec. Mysore Geol. Dep.*, 1913, **13**, 45.
4. Srinivasa Rao, M. R., *Mysore Geol Asso. Bull.*, 1956, **11**, 17.
5. Lemmlein, G. G. and Klevtsov, P. V., *Geochemistry*, 1961, **2**, 133.
6. Sourirajan, S. and Kennedy, G. C., *Am. J. Sci.*, 1962, **260**, 115.

ACKNOWLEDGEMENTS We thank Prof J. C. V. Shastri for encouragement and support during the investigation and CSIR, New Delhi, for financial assistance.

Received 8 July 1991; accepted 13 August 1991

Fluctuating sea levels off Bombay (India) between 14,500 and 10,000 years before present

Rajiv Nigam, N. H. Hashimi, Eileen T. Menezes and A. B. Wagh
National Institute of Oceanography, Dona Paula, Goa 403 004, India

A 26.5-metre-long core collected from the outer-shelf area off Bombay at 75 m water depth showed ooids and shallow-water benthic foraminifera all along the core. The presence of these well-known indicators of shallow-water environment of deposition shows that sea level had transgressed considerably prior to 10,000 years before present (^{14}C age of the surface sediment). By comparison with global events, we infer that the sea level was at 101.5 m below the present level at about 14,500 years BP. We further observe that this rise occurred with two minor pauses (or minor reversals) at 13,000 and 11,500 years BP.

GLOBAL variations of sea level are viewed in the light of their behaviour in the recent past and possible consequences of a future rise that may be accelerated by the greenhouse effect. There are evidences of sea level changes in the past few thousand years not only globally but also along the west coast of India. It is important to analyse the changes that took place over this region after the last glacial maximum[1] to understand the present and to anticipate the future.

It is known that sea level between 22,000 and 15,000 years before present (BP) was characterized by relatively stable conditions[1]. A number of studies[2–5] have been made on sea level at 10,000 years BP and the variations thereafter along the western continental shelf of India. However, the period before 10,000 years BP has not received adequate attention. Our objective in this study is to fill this gap.

We studied down-core variations of depth indicators like ooids and foraminifera in a bore-hole sample collected from the outer-shelf area off Bombay (19°02′10.44″N, 71°30′36.36″E) in the northern Arabian Sea (Figure 1). Depth of water at the bore-hole site is 75 m and the length of the core was 26.5 m.

The bore-hole sample was subsampled at one-metre intervals from 2 to 26.5 m. Approximately 200 g of subsamples from each level was brought to the laboratory and dried at 60°C. These samples were washed through a 230-mesh sieve (63 μm). The +63 μm fraction showed presence of ooids and shallow-water benthic foraminifera. Study of ooids in a core is important because they are indicators of low stands of sea level. They have earlier been reported from the surficial sediments of the western continental margin of India and their spatial distribution is well known[6–8]. The radiocarbon age has been reported to be between 9,000 and 11,000 years BP[8].

It was also recently observed that the zone on the shelf between 60 and 90 m, which has abundant ooids, also contains foraminiferal species like *Amphistegina*, *Operculina*, etc. These relict foraminiferal tests also showed the presence of the fouling barnacle species *Tetraclita squamosa*[11], which indicates prevalence of a high-salinity intertidal environment of deposition. This species is absent in the modern environment of the west coast of India, and therefore provides further conclusive evidence that the surficial sediment in the 60-to-90-m zone was deposited under shallow-water conditions.

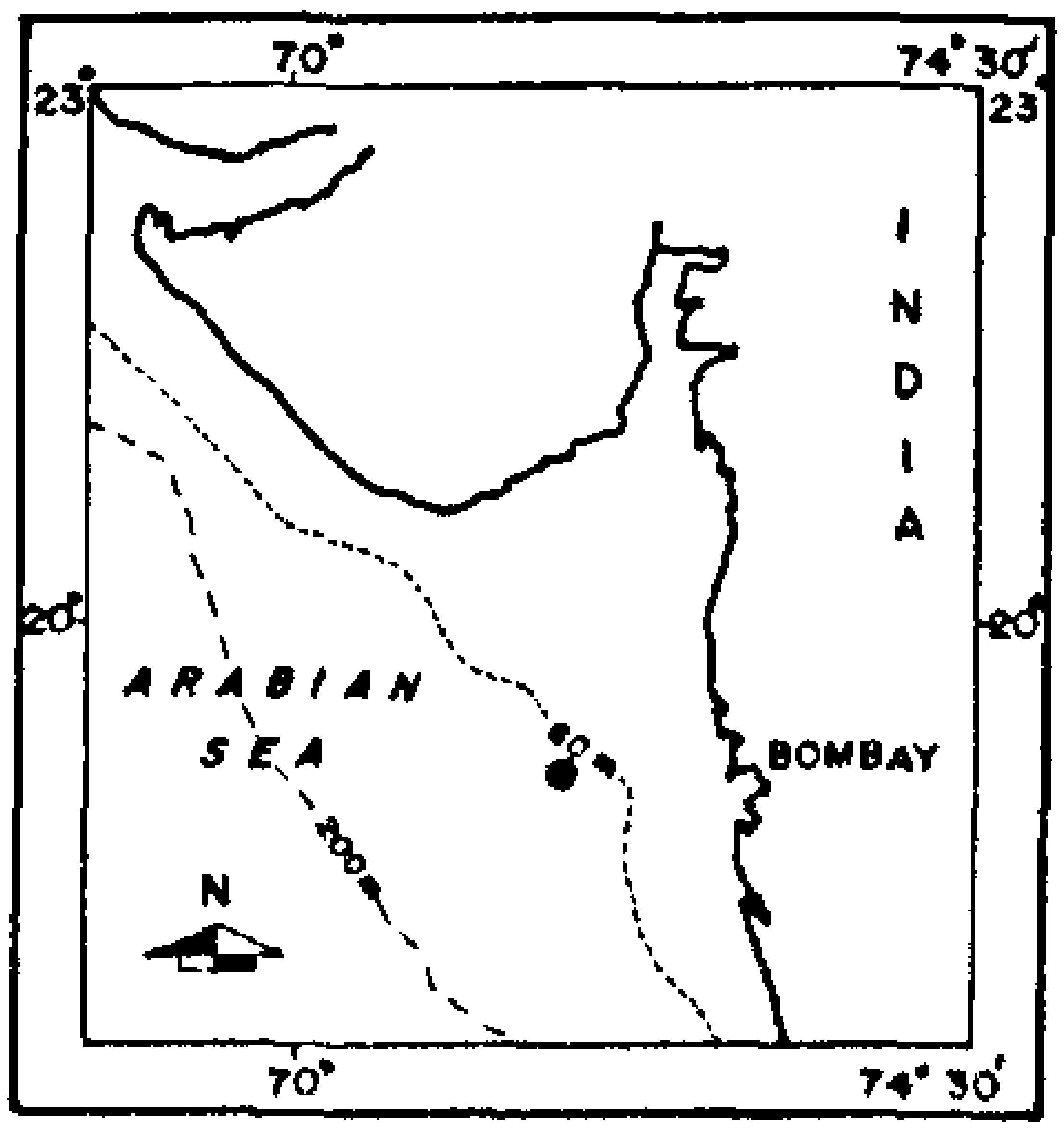

Figure 1. Location of bore-hole